J Neuropathol Exp Neurol

Vol. 65, No. 6
June 2006
pp. 540–548

ORIGINAL ARTICLE

Borrelia burgdorferi Induces TLR1 and TLR2 in Human Microglia and Peripheral Blood Monocytes but Differentially Regulates HLA-Class II Expression

Riccardo Cassiani-Ingoni, MS, Erik S. Cabral, MS, Jan D. Lünemann, MD, Zoila Garza, MS, Tim Magnus, MD, PhD, Harald Gelderblom, MD, Peter J. Munson, PhD, Adriana Marques, MD, and Roland Martin, MD

Abstract

The spirochete *Borrelia burgdorferi* is the agent of Lyme disease, which causes central nervous system manifestations in up to 20% of patients. We investigated the response of human brain microglial cells, glial progenitors, neurons, astrocytes, as well as peripheral blood monocytes to stimulation with *B. burgdorferi*. We used oligoarrays to detect changes in the expression of genes important for shaping adaptive and innate immune responses. We found that stimulation with *B. burgdorferi* lysate increased the expression of Toll-like receptors (TLRs) 1 and 2 in all cell types except neurons. However, despite similarities in global gene profiles of monocytes and microglia, only microglial cells responded to the stimulation with a robust increase in HLA-DR, HLA-DQ, and also coexpressed CD11-c, a dendritic cell marker. In contrast, a large number of HLA-related molecules were repressed at both the RNA and the protein levels in stimulated monocytes, whereas secretion of IL-10 and TNF-α was strongly induced. These results show that signaling through TLR1/2 in response to *B. burgdorferi* can elicit opposite immunoregulatory effects in blood and in brain immune cells, which could play a role in the different susceptibility of these compartments to infection.

From the Cellular Immunology Section (RCI, ESC, JDL, HG, RM), Neuroimmunology Branch, National Institute of Neurological Disorders and Stroke, Bethesda, Maryland; Mathematical and Statistical Computing Laboratory (ZG, PJM), Analytical Biostatistics Section, Center for Information Technology, Bethesda, Maryland; Stem Cell Biology Unit (TM), Laboratory of Neuroscience, National Institute on Aging, Bethesda, Maryland; Laboratory of Clinical Infectious Diseases (AM), National Institute of Allergy and Infectious Diseases, National Institutes of Health, Bethesda, Maryland; and Department of Human Physiology and Pharmacology (RCI), Center of Excellence in Biology and Molecular Medicine, University of Rome "La Sapienza," Rome, Italy.

Send correspondence and reprint requests to: Riccardo Cassiani-Ingoni, MS, Bldg.10, Room 5B06, 10 Center Drive, Bethesda, MD 20892; E-mail: cassianr@ninds.nih.gov

This research was supported in part by the Intramural Research Program of the National Institutes of Health, NINDS, NIAID, and NIMH. RCI is supported by the Integrative Neural Immune Program (INIP) of NIMH and is a doctoral candidate in the Research in Neurophysiology program at the University of Rome "La Sapienza."

Supplementary data is available online at http://www.jneuropath.com.

Key Words: Glia, HLA class II, Lyme disease, Microglia, Monocyte, Outer surface protein A, Toll-like receptor.

INTRODUCTION

Lyme disease is the most frequently occurring vector-borne infection in the United States and is also endemic in Europe and parts of Asia (1). Transmitted by *Ixodes* ticks, its causative agent *Borrelia burgdorferi* initially propagates locally in the skin before it disseminates hematogenously to other organ systems. Neurologic involvement occurs in up to 20% of patients and presents as cranial neuritis, meningoradiculitis, or encephalitis. Tissue tropism of *B. burgdorferi* for the nervous system and the inflammatory mechanisms that are involved in the local immune responses are at present only partly understood. The immune privilege of the central nervous system (CNS) and the functional characteristics of resident CNS cells likely play important roles.

In animal models of Lyme disease, CNS invasion leads to local tissue damage as a consequence of potent induction of proinflammatory mediators by microglial cells (2, 3). Microglia are resident immune cells within the CNS with a slow rate of turnover from circulating monocytes. When activated, microglial cells are capable of initiating a strong and prompt immune reaction against invading pathogens and orchestrate peripheral leukocyte infiltration (4). These responses are probably under tight spatial and temporal regulation, depending on the inducing stimulus/inflammatory context, to prevent immune-mediated brain damage. If activated in an uncontrolled fashion, microglial cells can amplify deleterious chronic immune responses within the CNS as suggested for cerebral malaria or multiple sclerosis (4, 5). Besides microglial cells, *B. burgdorferi*-mediated inflammation affects other glial and neuronal cells as well, which may occur directly through engagement of pattern recognition receptors expressed on these cells or indirectly as a result of mediator release from activated microglia. Pattern recognition receptors, which comprise the Toll-like receptors (TLR), can act as pathogen "sensors" by recognizing specific molecular structures that are conserved among members of each class of infectious agents. In this way, they confer

crucial information for shaping the specific immune response, for example, antibacterial as opposed to antiviral (6). TLR2 mediates immune responses to a broad range of microbial products and is critical for the recognition of bacterial lipopeptides or live infectious organisms (7); when it functions in combination with another member, TLR1, it can bind triacylated lipopeptides like mycobacterial lipoprotein and the outer surface protein A of *B. burgdorferi* (8, 9).

In vitro studies in murine microglia have shown that *B. burgdorferi* is capable of inducing the expression of pattern recognition receptors like TLR2 and CD14 in these cells (10), a critical step in immune activation in the CNS. Based on the potential impact of *B. burgdorferi*-induced cellular activation patterns for the human disease, it was important to investigate the cellular response of human brain and blood cells to these molecules. We stimulated microglia, astrocytes, neurons, and glial progenitors with *B. burgdorferi* in vitro. Using oligoarrays, we compared the individual cellular responses with that of peripheral blood monocytes in the same conditions. This analysis highlighted overlapping but characteristic expression profiles of monocytes and microglial cells as well as previously unrecognized differences in their response after TLR engagement.

MATERIALS AND METHODS

Isolation and Characterization of Brain Cells and Blood Monocytes

We used primary microglial cells, neuronal and glial progenitor cells isolated from human fetal tissue (ScienCell, San Diego, CA). Fluorescence-activated cell sorting (FACS) was used to further purify individual cell populations based on the expression of lineage-specific surface markers. We used antibodies against CD11-b (BD Biosciences, San Jose, CA) to sort microglial cells, A2B5 staining (Roche, Indianapolis, IN) for progenitors, and a mixture of tetanus toxin fragment C (TnTx) (Roche) together with a mouse monoclonal anti-TnTx antibody to sort neurons and neuronal progenitors, as previously described (11, 12). In culture, over 85% of neuronal cells were positive by antineurofilament (Chemicon, Temecula, CA) staining after 4 to 5 days. Pure populations of GFAP+ (Dako, Carpinteria, CA) astrocytes were differentiated in vitro from fetal neurospheres with 10% human serum (Gemini Bio Products, Woodland, CA) for 7 days. CD14-expessing peripheral monocytes were isolated from healthy volunteers by countercurrent elutriation from peripheral blood at the Department of Transfusion Medicine, Clinical Research Center, National Institutes of Health under a protocol approved by the National Cancer Institute Institutional Review Board, and all volunteers signed informed consent. Microglial cells and monocytes were cultured in IMDM (Gibco Invitrogen, Carlsbad, CA) with 3% human serum, glutamine, and antibiotics. The other brain cells were cultured in DMEM supplemented with 2% B-27 (both from Gibco Invitrogen) and antibiotics. Sorted populations were cultured in parallel in 6-well plates for at least 48 hours before stimulation with bacterial antigens to allow complete removal of the antibodies used for sorting as shown previously (13).

Stimulation with *Borrelia burgdorferi* Antigens

Stimulation with bacterial antigens was done using 1 μg/mL low-passage sonicate of *B. burgdorferi sensu stricto* strain B31 (Biodesign, Saco, ME) or with 0.1 μg/mL recombinant Lipidated-outer surface protein A (L-OspA) of *B. burgdorferi* (SmithKline Beecham Biologicals, Rixensart, Belgium). Antigen stimulation was performed in 2 mL fresh medium for 48 hours. No bacterial molecules were added in the control cultures. The final endotoxin concentration in medium for all antigens tested was <0.05 EU/mL (Endosafe-PTS) or <0.1 EU/mL (Cambrex Bioscience, East Rutherford, NJ). This time point and antigen concentration were chosen according to pilot time course and dose-titration experiments (data not shown) as well as published data using different cells (14, 15).

Oligoarray Hybridization

Total RNA was isolated with RNeasy (Qiagen, Valencia, CA) from parallel cultures of stimulated and unstimulated cells from individual donors. We independently hybridized RNA samples from a number of cell preparations of microglia (4 challenged, 3 mock), of monocytes (4 challenged, 3 control), neurons (1 challenged, 3 control), glial progenitors (2 challenged, 2 control), and astrocytes (1 challenged, 1 control). A minimum of 5 μg total RNA per cell preparation/condition was reverse-transcribed with T7-polyA primers (Invitrogen Life Technologies, Carlsbad, CA). In vitro transcription of cDNA was performed in the presence of biotinylated ribonucleotides (ENZO Diagnostics, New York, NY). Hybridization of 15 μg of cRNA to each Human Genome 133A GeneChip (Affymetrix, Santa Clara, CA) was done overnight. Secondary detection and scanning followed the manufacturer's protocols.

Statistical Analysis of Array Data

Affymetrix software GCOS version 1.2 was used to control the fluidics and scanners and to process raw intensity data into signal and present call values. Data were transferred and stored in the NIHLIMS database of Affymetrix microarray results. Data were analyzed using the MSCL Analyst's Toolbox (http://abs.cit.nih.gov) and the JMP statistical software (http://www.jmp.com). Signal values were retrieved, log10-transformed, and normalized to the median intensity of each chip. A principal components analysis (PCA) on the transformed data permitted visualization of the 24 samples in bivariate plots of the low-order principal components to detect possible outliers and to provide a global view of the study results.

The study included 5 cell types and 2 conditions (control and challenged). The response of microglia and monocytes (or the other cell types) was compared in a one-way analysis of variance with 4 levels. The p values were collected for each probe set and the corresponding false

discovery rate values computed. Log-fold change values were computed as the difference between the average stimulated (challenge) and unstimulated (mock) values for each cell type. Genes with >2-fold change in either direction, on either cell type, with a false discovery rate <10% were selected for further analysis. Two-way hierarchical clustering was performed on all 24 samples for a subset of 715 probe sets having high variability across samples (standard deviation above 0.7 in log10 units) and also having present calls in more than 3 samples. Hierarchical clustering was performed using Ward's method and JMP software. Colored heat maps give expression levels (above or below the mean level for each gene) as red or green, respectively.

Quantitative Reverse Transcriptase–Polymerase Chain Reaction

Total RNA was reverse-transcribed into cDNA with random hexamers using the TaqMan reverse transcription reagents per manufacturers instructions (Perkin Elmer, Boston, MA). Quantitative reverse transcriptase–polymerase chain reaction (RT-PCR) was performed on an ABI Prism 7700 Sequence Detection System (Perkin Elmer). Primers and probes were designed for detection of MyD88, TLR1, TLR2, TLR4, and TLR6 (Synthegen, Houston, TX) (Supplementary Table S2). For the detection of HLA-DR, IL-6, and GAPDH, we used Pre Developed Assay Reagents (Perkin Elmer). Gene expression was normalized to the levels of expression of GAPDH using the ΔΔ Ct method.

Fluorescence-Activated Cell Sorting Analysis of Monocytes and Microglia

Cells from stimulated and control cultures of monocytes or microglial cells were detached from the culture plates and stained for 30 minutes at 4°C using mouse monoclonal antibodies against the following human surface antigens: CD14 (M5E2), HLA-DQ (Tu169), HLA-DR (G46-6 or L243), CD11-c (HL3), and CD209 (DNC46) (all purchased from BD Biosciences, San Jose, CA) in addition to human TLR1 (GD2.F4) and TLR2 (TL2.1) (both from eBioscience, San Diego, CA). After 2 washes, median fluorescence intensity was measured using a FACSCalibur and data were analyzed using CellQuest software. Isotype-specific antibodies were used to set respective background.

Cytokine and Chemokine Protein Secretion Assays

Supernatants were collected from challenged and mock-incubated human monocytes and microglial cells (2×10^6 cells/2 mL medium/well) after 24 and 48 hours. This time point had been established as optimal in previous time course experiments. IFN-γ, TNF-α, IL-1β, IL-6, IL-10, IL-12, IL-15, and GM-CSF concentrations were determined with a Luminex100 cytometer (Luminex Corp., Austin, TX) using BioPlex Manager software (Bio-Rad Laboratories, Hercules, CA) and Lincoplex Cytokine Kits (Linco Research, St. Charles, MO) according to the manufacturer's instructions.

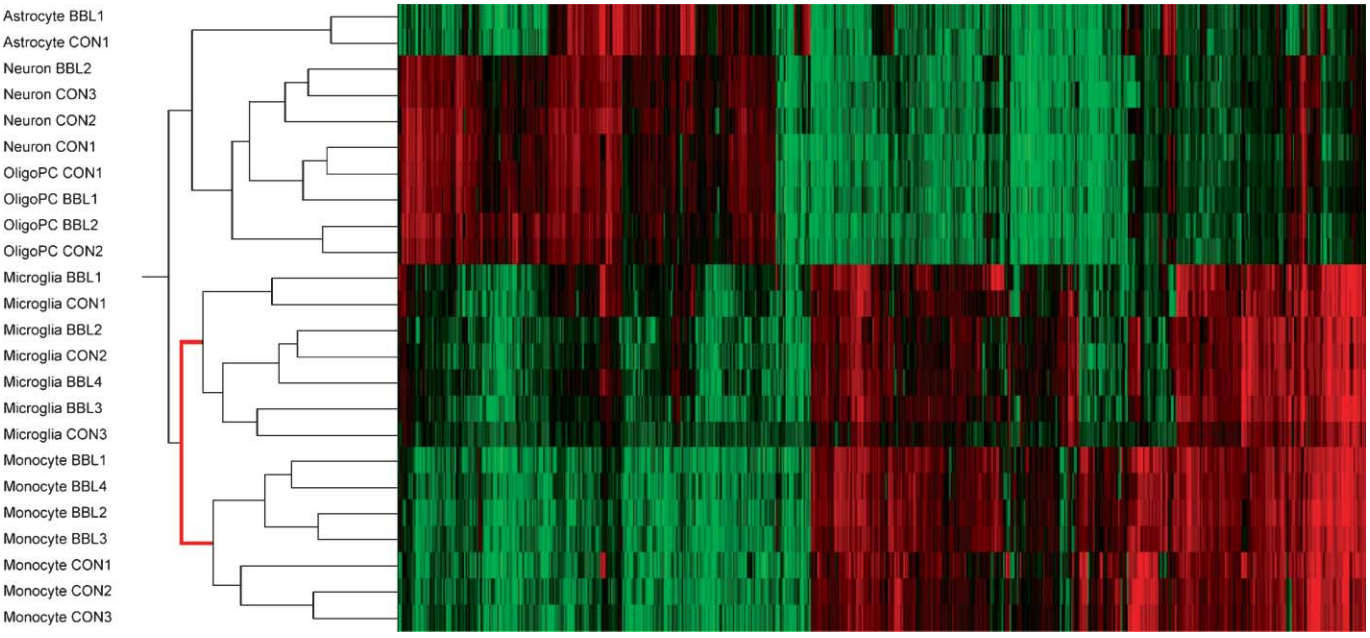

FIGURE 1. Microarray analysis of brain and blood cells after stimulation with *Borrelia burgdorferi*. Two-way hierarchical clustering was used to analyze samples comprising astrocytes, neurons, oligodendrocyte/glial progenitor cells, microglia, and peripheral monocytes stimulated with *B. burgdorferi* lysate (BBL) versus controls (CON). The resulting heat map visualizes the relative expression level measured for selected probe sets (see ''Materials and Methods'') within each sample, where red indicates an above-average and green a below-average response. Stimulated and control samples are accurately partitioned within each cell type. Microglia and monocytes cluster together and separate from all the other cell types.

RESULTS

Gene Expression of Brain Cells and Peripheral Monocytes in Response to *Borrelia burgdorferi*

Hierarchical cluster analysis was used to analyze gene-expression profiles (Fig. 1) of CD11-b+ microglial cells, A2B5+ glial progenitors, GFAP+ astrocytes, and neurofilament+ neuronal cells as well as CD14+ peripheral monocytes, stimulated with *B. burgdorferi* lysate. Clustering showed that monocytes and microglia grouped together separate from the other cell types. These similarities in global gene expression profiles between microglial cells and monocytes were expected in light of a similar immunologic function and of a common origin of these cells. Moreover, stimulation evoked changes in a greater number of genes in these 2 cell types compared with the others tested (not shown).

At the level of single genes or groups of genes, our initial analysis focused on the modulation of receptor molecules involved in innate immunity. We observed that the RNA for TLR2 was significantly upregulated in stimulated microglia and monocytes. Also, TLR1 was consistently up by an average of 1.5-fold in these cells. *B. burgdorferi* led to upregulation of both receptors also in astrocytes and glial progenitors, but not in neurons (not shown), suggesting that, among the TLRs, these 2 receptors could play a pivotal role in the response of all glial cell types in the event of CNS infection and on tissue injury.

TABLE 1. Summary of the Genes Whose Levels Were Significantly Changed at 48 Hours in Microglia and/or Monocytes After Stimulation With *Borrelia burgdorferi* Lysate Compared With Unstimulated Control Cells

Gene Category	Gene Symbol	Microglia	Monocyte
Toll-like receptors	TLR-2	↑+2.4	↑+3.2
Major histocompatibility complex, class II	CD74	=	↓+2.8↑
	MHC-II-TA	=	↓−6
	HLA-DPA1	=	↓−3.3
	HLA-DPB1	=	↓−3.4
	HLA-DQA1	=	↓−3.2
	HLA-DQB1	↓-2.1	↓−4.8
	HLA-DQB2	=	↓−2.1
	HLA-DRB3	=	↓−2.7
	HLA-DMA	=	↓−3.2
Chemokine	CXCL12	↑+2.0	=
	CCR7	↑+2.1	↑+2.0
	CX3CR1	=	↓−3.1
	CCR2	=	↑+4.2
	CXCL13	↓−2	↑+60
Others	IL1-R2	↑+6.4	↓−4.3
	PGDS	↓−2.4	−2
	NFKB2	↑+2	=
	MARCO	↑+6.3	↑+11.2
	TREM-1	=	↑+6.9
	CD44	=	↑+4
	SOCS-3	=	↑+19
	HSP-70	=	↑+2.1
	TREM-2	↓−2.1	↓−57

↑, Genes upregulated; =, genes not significantly changed; ↓, genes downregulated; numbers indicate the relative fold changes in expression.

Comparison of Gene Profiles Between Microglia and Monocytes

Understanding potential differences in the cellular response of monocytes and microglia to *B. burgdorferi* could provide insight into the CNS tissue-specific immune mechanisms. We thus focused our analysis on those genes that were up- or downregulated in stimulated microglia and/or monocytes compared with controls, leaving out all those genes that were not significantly changed in both cell types in response to the stimulus. Antigen stimulation evoked statistically significant, greater than 2-fold changes in 155 probe sets in microglial cells (93 up- and 62 downregulated) and in 308 probe sets in monocytes (171 up- and 137 downregulated); the full list of genes is provided as supplementary information (Supplementary Table S1). Table 1 provides a summary of the changes measured in genes encoding for TLRs, MHC class II-associated molecules, chemokines, and other molecules related to immune function; some of these molecules are further highlighted in the bivariate plot (Supplementary Fig. S1). We found that, although *B. burgdorferi* stimulation induced TLR2 transcription both in microglial cells and monocytes, the modulation of several MHC class II-related genes was very different. This stimulus induced a significant downmodulation of numerous HLA-associated genes only in monocytes, whereas these were not significantly altered (except for one) in microglial cells at 48 hours (Table and Supplementary Table S1). Among the differentially regulated genes were also members of the chemokine family and their receptors, which are particularly important in attracting immune cells to sites of inflammation and injury. In this context, the stimulation led to increased transcription of CXCL12 in microglia, but not in monocytes; in contrast, the RNA level of CXCL13 was highly increased in monocytes but decreased in microglia. These differences in response indicate that, under the same conditions, signaling through the TLR1/2 pathway in response to *B. burgdorferi* can elicit contrasting cell type-specific biologic changes in blood monocytes and brain microglial cells.

Changes in Toll-Like Receptor Expression Detected by Quantitative Polymerase Chain Reaction and Fluorescence-Activated Cell Sorting

To confirm at the mRNA and protein levels the changes measured by oligoarray, we analyzed TLR gene expression in microglia and monocytes using RT-PCR for selected receptors (TLR1, 2, 4, and 6) and for the adaptor molecule MyD88. We also used flow cytometry to compare TLR1 and TLR2 surface expression on resting versus stimulated cells. Besides stimulating monocytes and microglial cells with *B. burgdorferi* lysate, we used recombinant L-OspA, which is one of the major lipoproteins of this spirochete (8, 16). As shown in Figure 2A,

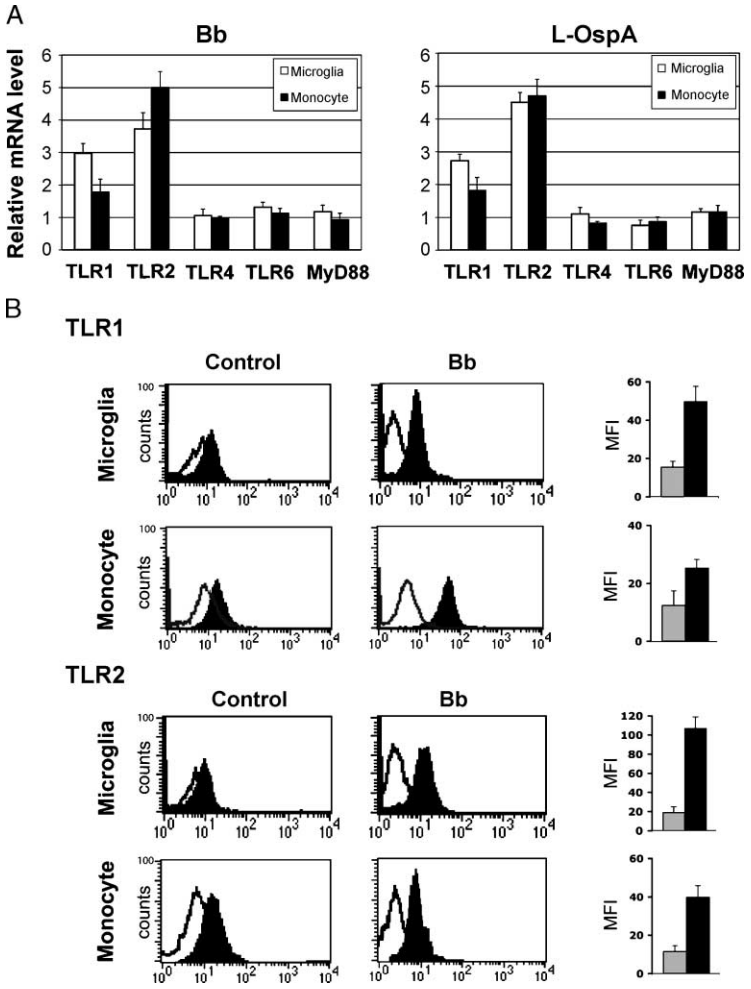

FIGURE 2. Modulation of Toll-like receptor (TLR) transcription and surface expression in stimulated microglia and monocytes. **(A)** Reverse transcriptase–polymerase chain reaction analysis of the mRNA levels of TLR1, TLR2, TLR4, TLR6, and MyD88 in microglia (white bars) and monocytes (black bars) after 48-hour stimulation with *Borrelia burgdorferi* lysate (left) or L-OspA (right) shows the induction of TLR1 and TLR2, but not of TLR4, TLR6, or MyD88, on both cells (n ≥3). **(B)** Representative fluorescence-activated cell sorting profiles of TLR1 and TLR2 surface expression on microglia and monocytes before and after *B. burgdorferi* stimulation show the increased expression of these receptors after stimulation. Open curves indicate fluorescent profiles of cells stained using isotype controls, as opposed to black curves for staining with the respective monoclonal antibodies. Bar graphs on the left summarize changes in mean fluorescent intensities (MFI) recorded in multiple experiments (n ≥3).

1 μg/mL *B. burgdorferi* lysate or 0.1 μg/mL L-OspA both induced a comparable 2-fold upregulation of TLR1 and a 3-fold upregulation of TLR2 gene expression at 48 hours in both monocytes and microglia. Both stimuli had no relevant effects (<2-fold change) on the expression of TLR4 (which recognizes lipopolysaccharide [LPS]) and TLR6 (which recognizes diacyl lipopeptides and lipoteichoic acid in conjunction with TLR2) or on the common signaling adaptor-protein MyD88 (which is shared by more than one TLR). The parallel induction of TLR1 and TLR2 gene expression in the 2 cell types was reflected by a robust increase in surface expression of both receptors as detected by flow cytometry (Fig. 2B).

Borrelia burgdorferi Induces MHC Class II Upregulation in Microglia but Downregulation in Monocytes

As revealed first by oligoarray analysis, only monocytes significantly downregulated several HLA-related gene transcripts within 48 hours. We sought to confirm these changes by measuring HLA-DR transcription using RT-PCR (Fig. 3A). We found that HLA-DR mRNA levels were strongly induced in microglial cells stimulated with *B. burgdorferi* or with L-OspA. In contrast, HLA-DR gene transcription was decreased in monocytes.

It should be noted that changes in gene expression do not always reflect parallel changes in protein expression. This is especially true for MHC class II molecules, which are readily mobilized from and then recycled to intracellular storage pools without a strict dependence on transcription. We thus analyzed by flow cytometry the levels of surface protein expression of HLA-DR, as well as of HLA-DQ, in resting and in *B. burgdorferi*-stimulated microglial cells and monocytes. Results of this analysis are shown in Figure 3B. We found that both HLA-DR and HLA-DQ molecules are expressed on unstimulated microglia and monocytes; baseline levels of expression are, however, lower on microglia, which reflects the very low expression level of MHC molecules in the nervous system. Surface expression of these molecules was clearly differentially regulated on stimulation. Although monocytes downregulated the expression of HLA molecules after challenge with *B. burgdorferi* lysate, or with L-OspA (not shown), either stimulus increased the expression of

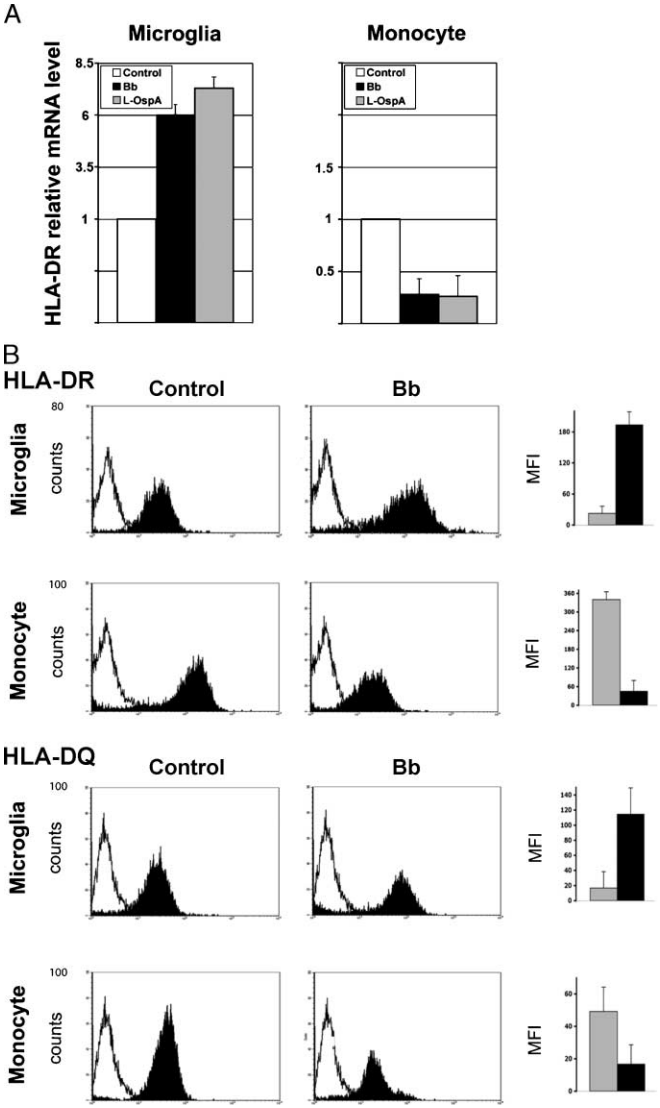

FIGURE 3. Modulation of HLA-DR and HLA-DQ expression in stimulated microglia and monocytes. **(A)** Reverse transcriptase–polymerase chain reaction analysis of HLA-DR mRNA levels in microglia and monocytes after stimulation with *Borrelia burgdorferi* (black bars) or L-OspA (gray bars) normalized to the levels measured in unstimulated cells (control, white bars) at 48 hours. Both stimuli induce a downregulation in the transcription of HLA-DR in monocytes but an upregulation in microglial cells. **(B)** Representative fluorescence-activated cell sorting profiles for HLA-DR and HLA-DQ on stimulated and unstimulated cells. Although stimulation with bacterial molecules increases the surface expression of HLA-DR and HLA-DQ on microglial cells, expression of both molecules is downregulated in monocytes. Bar graphs summarize changes in mean fluorescent intensities (MFI) recorded in multiple experiments (n ≥3).

HLA-DR and HLA-DQ in microglia. These results support the oligoarray data and further characterize the differential modulation of HLA-molecules in monocytes and microglial cells when stimulated by TLR agonists.

Borrelia burgdorferi Differentially Induces IL-10 and TNF-α in Monocytes and Microglia

Signaling through TLR1/2 can induce the release of autocrine factors that modulate the state of cellular activation through feedback mechanisms. We next investigated if differential cytokine production could account for the opposing effect of *B. burgdorferi* stimulation on MHC class II expression. Monocytes and microglia were stimulated with *B. burgdorferi* lysate 1 μg/mL for 24 and 48 hours, and levels of IFN-γ, TNF-α, IL-1β, IL-6, IL-10, IL-12, IL-15, and GM-CSF were measured in the supernatants. We found that monocytes produced 10 to 20 times higher amounts of IL-10 and TNF-α than microglia at both time points (Fig. 4). There were no differences in the production of the other cytokines. It is interesting that by microarray, only stimulated monocytes increased the expression of CXCL13 and SOCS-3 and downregulated MHC-II-TA (Table). Although these were all changes suggestive of IL-10 signaling in these cells (17–19), differences in IL-10 RNA were not detected.

Stimulated Microglial Cells Express Dendritic Cell Markers

The functional immunomodulatory role of microglial cells as brain dendritic cells received substantial attention

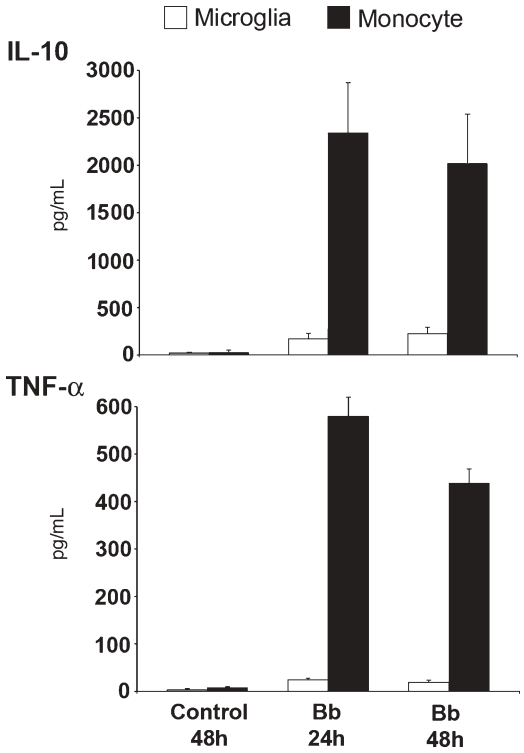

FIGURE 4. *Borrelia burgdorferi* induces robust secretion of IL-10 and TNF-α. Bars indicate the concentration of IL-10 (top) and TNF-α (bottom) in supernatants from microglial (white) and monocytic (black) cultures after 24 and 48 hours of stimulation compared with control cells at 48 hours. Under the same conditions, only monocytes secrete large amounts of both factors (n = 3).

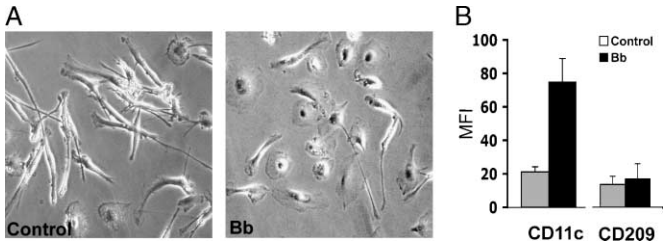

FIGURE 5. Expression of dendritic cell markers by microglia. **(A)** Morphologic changes in microglial cells stimulated with *Borrelia burgdorferi* lysate. **(B)** This stimulation induces the expression of CD11-c, but not of CD209, in a subset (20%) of CD11-b+ microglial cells as detected by flow cytometry (n = 3).

recently, especially in relation to inflammatory demyelinating conditions (20–22). The increased TLR and HLA expression in *B. burgdorferi*-stimulated microglial cells was accompanied by profound changes in cellular morphology (Fig. 5A). Stimulated microglial cells lost the characteristic elongated morphology to become more round with radial processes that was reminiscent of those of blood dendritic cells in culture. Next, we asked whether microglial cells stimulated with *B. burgdorferi* could acquire the expression of dendritic cell markers, namely CD11-c or CD209 (DC-SIGN), as determined by flow cytometry. TLR1/2 stimulation induced a robust expression of CD11-c on approximately 20% of all CD11-b+ microglial cells. In contrast, we did not detect CD209 on microglial and both molecules were absent on stimulated and unstimulated monocytes.

These data indicate that a subset of microglial cells could acquire dendritic cell functions after TLR stimulation by bacterial antigens.

DISCUSSION

Infiltration of the spirochete *B. burgdorferi* from the blood into the CNS compartment in patients with Lyme disease is associated with inflammation of the meninges, nerve roots, or the brain and spinal cord, which result in the clinical manifestations of neuroborreliosis. Because nervous system manifestations of Lyme disease occur frequently, besides the chronic involvement of the skin, the heart, and the joints, and because the CNS is considered an immunoprivileged organ, it is important to understand which factors contribute to tissue inflammation in the CNS. Although adaptive immune responses by T cells and antibodies have received most attention in the past in this context, it has become clear that the recognition of microbial molecular patterns by innate immune mechanisms plays an important role not only during acute inflammation, but also in shaping adaptive immune responses. After their initial characterization in *Drosophila*, the functional importance of TLRs for the recognition of bacterial and viral antigens, as well as of endogenous molecules associated with tissue damage, has been recognized also in mammalian cells (23, 24). Signaling through these receptors influences and finely tunes both innate and adaptive immune responses by controlling the state of activation of antigen presenting cells, scavenger cells, and lymphocytes, and possibly many other cell types as well. A number of TLRs are expressed in the normal human brain (25). Upregulation of specific receptors has been demonstrated in mouse microglial cells and astrocytes exposed to inflammatory signals (14,26). TLR2, in particular, together with a number of different chemokines and cytokines, appears to play an important role in the pathogenesis of Lyme disease both in humans and in experimental models (27–29).

Interestingly, we found that TLR2 is upregulated on microglial cells, astrocytes, glial progenitors, but not in neurons, in response to stimulation *B. burgdorferi*. On one hand, this indicates that all 3 cell types express the molecular machinery that allows them to bind and react to signals of "danger" released by invading pathogens as well as by the injured tissue itself. It was particularly interesting to challenge glial progenitor cells, which are generally identified in the adult brain by surface coexpression of A2B5 and NG2 antigens, because these cells become rapidly activated, divide, and migrate extensively in response to tissue damage and inflammation (30). However, a direct influence of bacterial molecules on progenitors through the TLR pathway had not been previously investigated. Because TLR2 can also bind the hydrophilic portions of endogenous molecules that are released by dead cells in the injured tissue (31), this receptor could play a broader role in activating glial cells in the surrounding areas and/or guiding them to the damaged sites of the CNS. On the other hand, progenitor cells could also be actively involved in the orchestration of brain's immune response.

Because *B. burgdorferi* disseminates mainly through the bloodstream, it was important to include monocytes in our analysis and to compare the expression profiles of blood cells with those of brain cells. Microglial cells and monocytes showed comparable gene expression profiles and clustered together both in resting conditions and on stimulation. Also, a greater number of genes were changed by *B. burgdorferi* stimulation in monocytes and microglia compared with the other cells (not shown), consistent with the notion that microglial cells constitute the first line of immune surveillance in the brain. A closer look, however, revealed important differences in their response to stimulation.

The downregulation of numerous HLA molecules seen only in monocytes was striking. Interestingly, some research suggests that certain pathogens might use TLR signaling to their own benefit (32), besides serving the host's immune cells as molecular pattern receptors. Activation of the TLR1/2 pathway could help induce a state of tolerance in some tissues, thereby suppressing the inflammatory reaction that would otherwise eliminate the pathogen (33, 34). A similar suppression has been described in monocytes stimulated with *Mycobacterium tuberculosis* (35), which in turn decreased the proinflammatory responsiveness of these cells to interferon-γ (36) as well as antigen-processing and presentation to T-lymphocytes (37, 38). It has been suggested that *B. burgdorferi* may also avoid immune surveillance by cell-associated persistence (39–41) and/or by avoiding complement-mediated

killing (42–44) through a variety of mechanisms. Down-modulation of HLA molecules on peripheral monocytes by contact with *B. burgdorferi* antigens could represent an important factor in immune evasion by this organism.

Although the inhibitory effect on HLA expression on monocytes was proposed to be TLR2-dependent in experiments using *Mycobacterium* (37), the differential modulation of this gene family shown by microglia indicated an influence on HLA class II expression by pathways downstream of TLR signaling. We found that IL-10 and TNF-α, 2 molecules that can induce a state of tolerance in monocytes (34, 36, 45) and repress MHC expression when released in response to antigenic stimulation (46, 47), were robustly induced in monocytes in response to *B. burgdorferi*. Consistent with autocrine effects of IL-10, the levels of some of its known targets were changed; by microarray, only monocytes increased the expression of CXCL13 and SOCS-3 and decreased MHC class II transactivator, which are all known changes induced by IL-10 (17–19). We therefore suggest that the opposing effects on HLA class II regulation are at least partially mediated by differential secretion of these factors in response to *B. burgdorferi*. Further investigation of these molecular pathways is clearly of interest in the context of immune evasion by human pathogens, and the direct comparison of the responses of monocytes and microglia in vitro can serve as a useful model to address some of these questions.

Among the genes encoding for chemokines that were differentially induced or repressed in the 2 cell types, CXCL12 (stromal derived factor-1α [SDF-1α]) was the only chemokine transcript significantly upregulated in microglia. This observation is interesting because elevated levels CXCL12 have been detected in the cerebrospinal fluid of patients with Lyme neuroborreliosis (48). Furthermore, CXCL12 is known to direct dendritic cells as well as neural/glial progenitor cells to sites of injury in the CNS (48–50), which can stimulate tissue repair as well. Microglial cells probably represent an important source of this chemokine in vivo. On the other hand, CXCL13 (B-cell-attracting chemokine-1 [BCA-1]) was the only chemokine increased in monocytes but downregulated in microglia. This molecule has been previously associated with *B. burgdorferi* infection of peripheral tissues in a primate model of Lyme disease where it might modulate peripheral antibody-mediated responses to the spirochete (2). Moreover, CXCL13 is also a putative diagnostic marker for Lyme neuroborreliosis (51, 52).

Microglial cells stimulated with *B. burgdorferi* showed profound changes in morphology, resulting in the acquisition of a more round cellular shape, elevated surface levels of HLA-DR and HLA-DQ molecules, and increased secretion of IL-6 (not shown; which has also been detected at high levels in the CNS in Lyme disease [53]). In this context, microglial cells might rapidly acquire function as antigen-presenting cells in the brain and further stimulate the inflammatory response (54, 55). Interestingly, we found that a subpopulation of microglial cells acquired expression of CD11-c, a marker of dendritic cells that is known to interact with a diverse repertoire of ligands, including CD23 expressed by activated B-lymphocytes and blood dendritic cells. These results mirror previous observations on immature blood dendritic cells, showing that some bacterial products can stimulate their differentiation toward a more mature phenotype (56–58). Maturation of microglial cells could allow for efficient antigen presentation in the brain parenchyma, which is necessary for mounting a locally confined immune response against the spirochete.

We are currently investigating the relevance of these patterns of activation in vivo by analyzing the brains of mice infected with a neurotropic strain of *Borrelia*. Interestingly enough, CNS infection was accompanied by widespread glial activation, together with increased TLR1 and TLR2 expression (unpublished data). Future work will aim at elucidating the contribution of the TLR1/2 pathway in the pathogenesis of neuroborreliosis.

ACKNOWLEDGMENT

The authors thank Ronald Hornung for performing the Luminex assays.

REFERENCES

1. Steere AC, Coburn J, Glickstein L. The emergence of Lyme disease. J Clin Invest 2004;113:1093–101
2. Pachner AR, Dail D, Narayan K, et al. Increased expression of B-lymphocyte chemoattractant, but not pro-inflammatory cytokines, in muscle tissue in rhesus chronic Lyme borreliosis. Cytokine 2002;19: 297–307
3. Isogai E, Isogai H, Kimura K, et al. Cytokines in the serum and brain in mice infected with distinct species of Lyme disease *Borrelia.* Microb Pathog 1996;21:413–19
4. Aloisi F. Immune function of microglia. Glia 2001;36:165–79
5. Benveniste EN. Role of macrophages/microglia in multiple sclerosis and experimental allergic encephalomyelitis. J Mol Med 1997;75:165–73
6. Iwasaki A, Medzhitov R. Toll-like receptor control of the adaptive immune responses. Nat Immunol 2004;5:987–95
7. Lien E, Sellati TJ, Yoshimura A, et al. Toll-like receptor 2 functions as a pattern recognition receptor for diverse bacterial products. J Biol Chem 1999;274:33419–25
8. Alexopoulou L, Thomas V, Schnare M, et al. Hyporesponsiveness to vaccination with *Borrelia burgdorferi* OspA in humans and in TLR1- and TLR2-deficient mice. Nat Med 2002;8:878–84
9. Takeuchi O, Sato S, Horiuchi T, et al. Cutting edge: role of Toll-like receptor 1 in mediating immune response to microbial lipoproteins. J Immunol 2002;169:10–14
10. Rasley A, Anguita J, Marriott I. *Borrelia burgdorferi* induces inflammatory mediator production by murine microglia. J Neuroimmunol 2002;130:22–31
11. Maric D, Maric I, Barker JL. Flow cytometric strategies to study CNS development. In: Boulton AA, Baker GB, eds. *Neuromethods.* Totowa, NJ: Humana, 1999:287–318
12. Maric D, Maric I, Barker JL. Developmental changes in cell calcium homeostasis during neurogenesis of the embryonic rat cerebral cortex. Cereb Cortex 2000;10:561–73
13. Wu YY, Mujtaba T, Han SS, et al. Isolation of a glial-restricted tripotential cell line from embryonic spinal cord cultures. Glia 2002;38:65–79
14. Olson JK, Miller SD. Microglia initiate central nervous system innate and adaptive immune responses through multiple TLRs. J Immunol 2004;173:3916–24
15. Carpentier PA, Begolka WS, Olson JK, et al. Differential activation of astrocytes by innate and adaptive immune stimuli. Glia 2005;49:360–74
16. Haupl T, Landgraf S, Netusil P, et al. Activation of monocytes by three OspA vaccine candidates: Lipoprotein OspA is a potent stimulator of monokines. FEMS Immunol Med Microbiol 1997;19:15–23

17. Donnelly RP, Dickensheets H, Finbloom DS. The interleukin-10 signal transduction pathway and regulation of gene expression in mononuclear phagocytes. J Interferon Cytokine Res 1999;19:563–73
18. Perrier P, Martinez FO, Locati M, et al. Distinct transcriptional programs activated by interleukin-10 with or without lipopolysaccharide in dendritic cells: Induction of the B cell-activating chemokine, CXC chemokine ligand 13. J Immunol 2004;172:7031–42
19. Yee CS, Yao Y, Xu Q, et al. Enhanced production of IL-10 by dendritic cells deficient in CIITA. J Immunol 2005;174:1222–29
20. Greter M, Heppner FL, Lemos MP, et al. Dendritic cells permit immune invasion of the CNS in an animal model of multiple sclerosis. Nat Med 2005;11:328–34
21. Suter T, Malipiero U, Otten L, et al. Dendritic cells and differential usage of the MHC class II transactivator promoters in the central nervous system in experimental autoimmune encephalitis. Eur J Immunol 2000;30:794–802
22. McMahon EJ, Bailey SL, Castenada CV, et al. Epitope spreading initiates in the CNS in two mouse models of multiple sclerosis. Nat Med 2005;11:335–39
23. Akira S, Hemmi H. Recognition of pathogen-associated molecular patterns by TLR family. Immunol Lett 2003;85:85–95
24. Morr M, Takeuchi O, Akira S, et al. Differential recognition of structural details of bacterial lipopeptides by toll-like receptors. Eur J Immunol 2002;32:3337–47
25. Bsibsi M, Ravid R, Gveric D, et al. Broad expression of Toll-like receptors in the human central nervous system. J Neuropathol Exp Neurol 2002;61:1013–21
26. Ebert S, Gerber J, Bader S, et al. Dose-dependent activation of microglial cells by Toll-like receptor agonists alone and in combination. J Neuroimmunol 2005;159:87–96
27. Hirschfeld M, Kirschning CJ, Schwandner R, et al. Cutting edge: inflammatory signaling by *Borrelia burgdorferi* lipoproteins is mediated by toll-like receptor 2. J Immunol 1999;163:2382–86
28. Thomas V, Fikrig E. The Lyme disease vaccine takes its toll. Vector Borne Zoonotic Dis 2002;2:217–22
29. Wang G, Ma Y, Buyuk A, et al. Impaired host defense to infection and Toll-like receptor 2-independent killing of *Borrelia burgdorferi* clinical isolates in TLR2-deficient C3H/HeJ mice. FEMS Microbiol Lett 2004; 231:219–25
30. Chen ZJ, Negra M, Levine A, et al. Oligodendrocyte precursor cells: reactive cells that inhibit axon growth and regeneration. J Neurocytol 2002;31:481–95
31. Seong SY, Matzinger P. Hydrophobicity: An ancient damage-associated molecular pattern that initiates innate immune responses. Nat Rev Immunol 2004;4:469–78
32. Matzinger P. The danger model: A renewed sense of self. Science 2002; 296:301–305
33. Chiao JW, Pavia C, Riley M, et al. Antigens of Lyme disease of spirochaete *Borrelia burgdorferi* inhibits antigen or mitogen-induced lymphocyte proliferation. FEMS Immunol Med Microbiol 1994;8:151–55
34. Diterich I, Rauter C, Kirschning CJ, et al. *Borrelia burgdorferi*-induced tolerance as a model of persistence via immunosuppression. Infect Immun 2003;71:3979–87
35. Noss EH, Harding CV, Boom WH. *Mycobacterium tuberculosis* inhibits MHC class II antigen processing in murine bone marrow macrophages. Cell Immunol 2000;201:63–74
36. Fortune SM, Solache A, Jaeger A, et al. *Mycobacterium tuberculosis* inhibits macrophage responses to IFN-gamma through myeloid differentiation factor 88-dependent and -independent mechanisms. J Immunol 2004;172:6272–80
37. Noss EH, Pai RK, Sellati TJ, et al. Toll-like receptor 2-dependent inhibition of macrophage class II MHC expression and antigen processing by 19-kDa lipoprotein of *Mycobacterium tuberculosis.* J Immunol 2001;167:910–18
38. Gehring AJ, Rojas RE, Canaday DH, et al. The *Mycobacterium tuberculosis* 19-kilodalton lipoprotein inhibits gamma interferon-regulated HLA-DR and Fc gamma R1 on human macrophages through Toll-like receptor 2. Infect Immun 2003;71:4487–97
39. Montgomery RR, Nathanson MH, Malawista SE. The fate of *Borrelia burgdorferi*, the agent for Lyme disease, in mouse macrophages. Destruction, survival, recovery. J Immunol 1993;150:909–15
40. Girschick HJ, Huppertz HI, Russmann H, et al. Intracellular persistence of *Borrelia burgdorferi* in human synovial cells. Rheumatol Int 1996; 16:125–32
41. Klempner MS, Noring R, Rogers RA. Invasion of human skin fibroblasts by the Lyme disease spirochete, *Borrelia burgdorferi.* J Infect Dis 1993;167:1074–81
42. Liang FT, Jacobs MB, Bowers LC, et al. An immune evasion mechanism for spirochetal persistence in Lyme borreliosis. J Exp Med 2002;195:415–22
43. Bubeck-Martinez S. Immune evasion of the Lyme disease spirochetes. Front Biosci 2005;10:873–78
44. Kraiczy P, Skerka C, Kirschfink M, et al. Immune evasion of *Borrelia burgdorferi*: insufficient killing of the pathogens by complement and antibody. Int J Med Microbiol 2002;291(suppl 33):141–46
45. Wolk K, Kunz S, Crompton NE, et al. Multiple mechanisms of reduced major histocompatibility complex class II expression in endotoxin tolerance. J Biol Chem 2003;278:18030–36
46. Jasinski M, Wieckiewicz J, Ruggiero I, et al. Isotype-specific regulation of MHC class II gene expression in human monocytes by exogenous and endogenous tumor necrosis factor. J Clin Immunol 1995;15:185–93
47. Kowalczyk D, Mytar B, Jasinski M, et al. Modulation of monocyte antigen-presenting capacity by tumour necrosis factor-alpha (TNF): Opposing effects of exogenous TNF before and after an antigen pulse and the role of TNF gene activation in monocytes. Immunol Lett 1995; 44:51–57
48. Pashenkov M, Teleshova N, Kouwenhoven M, et al. Recruitment of dendritic cells to the cerebrospinal fluid in bacterial neuroinfections. J Neuroimmunol 2002;122:106–16
49. Imitola J, Raddassi K, Park KI, et al. Directed migration of neural stem cells to sites of CNS injury by the stromal cell-derived factor 1alpha/CXC chemokine receptor 4 pathway. Proc Natl Acad Sci U S A 2004;101:18117–22
50. Dziembowska M, Tham TN, Lau P, et al. A role for CXCR4 signaling in survival and migration of neural and oligodendrocyte precursors. Glia 2005;50:258–69
51. Segal BM, Logigian EL. Sublime diagnosis of Lyme neuroborreliosis. Neurology 2005;65:351–52
52. Rupprecht TA, Pfister HW, Angele B, et al. The chemokine CXCL13 (BLC): A putative diagnostic marker for neuroborreliosis. Neurology 2005;65:448–50
53. Pachner AR, Amemiya K, Delaney E, et al. Interleukin-6 is expressed at high levels in the CNS in Lyme neuroborreliosis. Neurology 1997;49: 147–52
54. Fischer HG, Bonifas U, Reichmann G. Phenotype and functions of brain dendritic cells emerging during chronic infection of mice with *Toxoplasma gondii.* J Immunol 2000;164:4826–34
55. Fischer HG, Reichmann G. Brain dendritic cells and macrophages/microglia in central nervous system inflammation. J Immunol 2001;166:2717–26
56. O'Doherty U, Ignatius R, Bhardwaj N, et al. Generation of monocyte-derived dendritic cells from precursors in rhesus macaque blood. J Immunol Methods 1997;207:185–94
57. Kokkinopoulos I, Jordan WJ, Ritter MA. Toll-like receptor mRNA expression patterns in human dendritic cells and monocytes. Mol Immunol 2005;42:957–68
58. Suhonen J, Komi J, Soukka J, et al. Interaction between *Borrelia burgdorferi* and immature human dendritic cells. Scand J Immunol 2003;58:67–75

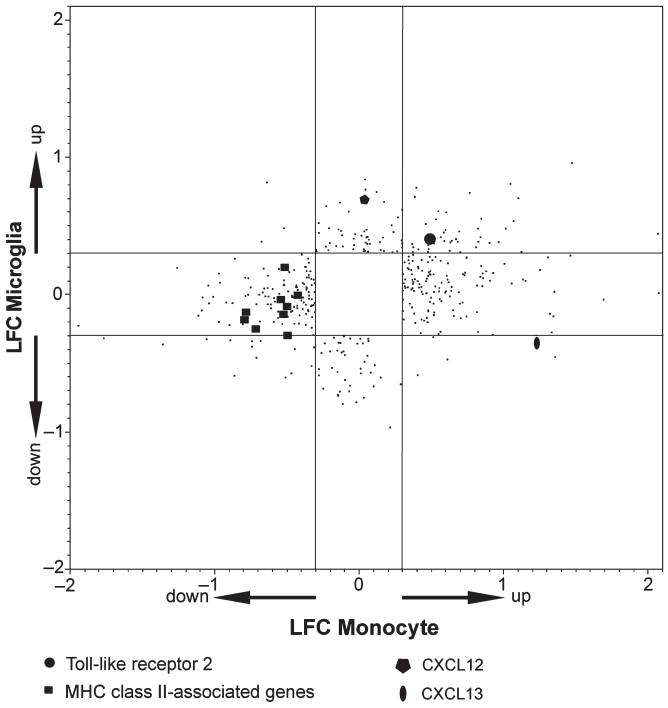

Supplementary Figure 1.

Table S1: **Changes in gene expression in monocytes and microglia following stimulation with *B. burgdorferi*.** Probe ID's that met a statistical significant >2-fold change in expression were grouped by combination of logarithmic fold change (LFC) in monocytes (MC) and logarithmic fold change in microglia (MG). The top table summarizes the total number of probes identified for every group.
The bottom list provides gene titles, gene symbols, statistical p-value, ratio of LFC-MG/LFC-MC and the group for each probe ID; U= up-regulated, 0= not changed, D= down-regulated. Within each group, gene symbols are listed in alphabetical order.

Indicator-LFC-Monocyte	Indicator-LFC-Microglia	Number of Probe ID's
Down	Down	16
Down	No Change	118
Down	Up	3
No Change	Down	40
No Change	Up	46
Up	No Change	121
Up	Up	44
Up	Down	6

Title	Gene Symbol	p (4 level ANOVA)	LFC-MG/MC	Group
Homo sapiens cDNA FLJ26905 fis, clone RCT01427	---	5.77E-08	-1.8925269	MC - 0 , MG - D
Homo sapiens transcribed sequences	---	0.00124764	-0.2624357	MC - 0 , MG - D
Homo sapiens LOC347025 (LOC347025), mRNA	---	0.00223043	0.17671549	MC - 0 , MG - D
Homo sapiens hypothetical protein PRO2133	---	0.00142349	0.4524973	MC - 0 , MG - D
Homo sapiens cDNA FLJ13453 fis, clone PLACE1003205.	---	0.0010009	0.52696234	MC - 0 , MG - D
hypothetical protein CG003	13CDNA73	0.00382702	-0.9573589	MC - 0 , MG - D
ATP-binding cassette, sub-family B (MDR/TAP), member 11	ABCB11	0.00101418	0.67138969	MC - 0 , MG - D
adenylate cyclase 9	ADCY9	0.00018567	-0.936658	MC - 0 , MG - D
butyrobetaine (gamma), 2-oxoglutarate dioxygenase (gamma-butyrobetaine hydroxylase) 1	BBOX1	0.00204098	-0.363348	MC - 0 , MG - D
chemokine binding protein 2	CCBP2	0.00303436	-0.3011484	MC - 0 , MG - D
carboxylesterase 1 (monocyte/macrophage serine esterase 1)	CES1	0.00359578	-0.7075256	MC - 0 , MG - D
cysteine-rich protein 1 (intestinal)	CRIP1	0.00002997	-1.0902271	MC - 0 , MG - D
DNA segment on chromosome 12 (unique) 2489 expressed sequence	D12S2489E	0.0000236	-0.9065316	MC - 0 , MG - D
dipeptidase 1 (renal)	DPEP1	0.00144025	-0.2877782	MC - 0 , MG - D

dipeptidylpeptidase 4 (CD26, adenosine deaminase complexing protein 2)	DPP4	0.00012239	0.61719168	MC - 0 , MG - D
endothelin receptor type A	EDNRA	0.00270664	0.36550132	MC - 0 , MG - D
family with sequence similarity 12, member A	FAM12A	0.00080059	-0.3290031	MC - 0 , MG - D
fibroblast growth factor receptor substrate 3	FRS3	0.00281435	-0.1063258	MC - 0 , MG - D
glycophorin A (includes MN blood group)	GYPA	0.00023914	0.30289671	MC - 0 , MG - D
hydroxysteroid (17-beta) dehydrogenase 2	HSD17B2	0.00106545	0.45183952	MC - 0 , MG - D
insulin-like growth factor 1 (somatomedin C)	IGF1	0.00017283	1.33917402	MC - 0 , MG - D
immunoglobulin lambda joining 3	IGLJ3	0.00000105	-1.4623561	MC - 0 , MG - D
IGF-II mRNA-binding protein 2	IMP-2	0.00245742	-0.405917	MC - 0 , MG - D
iroquois homeobox protein 5	IRX5	0.00273676	0.19569992	MC - 0 , MG - D
integrin, alpha 4 (antigen CD49D, alpha 4 subunit of VLA-4 receptor)	ITGA4	0.00002033	-1.1204005	MC - 0 , MG - D
KIAA1102 protein	KIAA1102	0.00162067	0.60484403	MC - 0 , MG - D
lysosomal apyrase-like protein 1	LALP1	0.00317948	-0.283572	MC - 0 , MG - D
lymphoid enhancer-binding factor 1	LEF1	0.00242489	0.43711777	MC - 0 , MG - D
melanoma antigen, family A, 12	MAGEA12	0.00362535	-0.3257423	MC - 0 , MG - D
myelin-associated oligodendrocyte basic protein	MOBP	0.00242143	-0.1000405	MC - 0 , MG - D
nucleosome assembly protein 1-like 2	NAP1L2	0.00140177	-0.3218116	MC - 0 , MG - D
nuclear receptor subfamily 2, group E, member 1	NR2E1	0.0025455	0.04299233	MC - 0 , MG - D
pellino homolog 2 (Drosophila)	PELI2	0.00184669	-0.7165658	MC - 0 , MG - D
placenta-specific 4	PLAC4	0.00002923	0.18340446	MC - 0 , MG - D
perforin 1 (pore forming protein)	PRF1	0.00192071	-0.6567171	MC - 0 , MG - D
regulator of G-protein signalling 1	RGS1	0.0013057	1.06587441	MC - 0 , MG - D
ring finger protein 128	RNF128	0.00268006	0.6826285	MC - 0 , MG - D
solute carrier family 22 (organic cation transporter), member 17	SLC22A17	0.00101243	0.54067803	MC - 0 , MG - D
T-cell leukemia/lymphoma 6	TCL6	0.00047069	0.35985764	MC - 0 , MG - D
T cell receptor gamma locus	TRG@	0.00037555	-0.6064981	MC - 0 , MG - D
Homo sapiens, clone IMAGE:5728597, mRNA	---	0.00021749	-0.7913305	MC - 0 , MG - U
Homo sapiens clone H2-38 anti-oxidized LDL immunoglobulin light chain Fab mRNA	---	0.00007701	-1.4066914	MC - 0 , MG - U
Homo sapiens hypothetical protein FLJ20234	---	0.00005165	-1.057876	MC - 0 , MG - U
HBG_HUMAN Hemoglobin gamma-A and gamma-G chains	---	0.00064235	-0.5437002	MC - 0 , MG - U
Homo sapiens cDNA: FLJ20908 fis, clone ADSE00417	---	0.00310798	0.67062164	MC - 0 , MG - U
Homo sapiens hypothetical protein FLJ11267 [Homo sapiens]	---	0.00026127	-0.4094819	MC - 0 , MG - U
B-cell CLL/lymphoma 7C	BCL7C	0.00356744	-0.6335339	MC - 0 , MG - U
chromosome 16 open reading frame 7	C16orf7	0.00125466	-0.2918126	MC - 0 , MG - U
complement component 1, q subcomponent, beta polypeptide	C1QB	0.0000338	1.4741688	MC - 0 , MG - U
cyclin D1 (PRAD1: parathyroid adenomatosis 1)	CCND1	0.00383324	0.86063086	MC - 0 , MG - U

CD2 antigen (cytoplasmic tail) binding protein 2	CD2BP2	0.00157699	-0.3241037	MC - 0 , MG - U
clathrin, heavy polypeptide (Hc)	CLTC	0.00363635	-0.4520574	MC - 0 , MG - U
crystallin, mu	CRYM	0.00202517	-0.3425332	MC - 0 , MG - U
chemokine (C-X-C motif) ligand 12 (stromal cell-derived factor 1)	CXCL12	0.00264491	0.43812887	MC - 0 , MG - U
chemokine (C-X-C motif) ligand 12 (stromal cell-derived factor 1)	CXCL12	0.00010199	1.37352859	MC - 0 , MG - U
hypothetical protein, estradiol-induced	E2IG4	0.00151878	0.69637916	MC - 0 , MG - U
EH-domain containing 1	EHD1	0.00134252	-0.2066672	MC - 0 , MG - U
eukaryotic translation initiation factor 4A, isoform 1	EIF4A1	0.00154031	-0.3352194	MC - 0 , MG - U
fibroblast growth factor 18	FGF18	0.00256249	0.02294072	MC - 0 , MG - U
hypothetical protein FLJ35827	FLJ35827	0.00105274	-0.537032	MC - 0 , MG - U
forkhead box M1	FOXM1	0.00038078	0.57195419	MC - 0 , MG - U
G protein-coupled receptor kinase 6	GPRK6	0.00069154	-0.3804376	MC - 0 , MG - U
KIAA0233 gene product	KIAA0233	0.00035295	-0.5874706	MC - 0 , MG - U
KIAA0540 protein	KIAA0540	0.00049592	-1.0447935	MC - 0 , MG - U
KIAA0763 gene product	KIAA0763	0.00022611	-0.5718674	MC - 0 , MG - U
KIAA0889 protein	KIAA0889	0.00005049	-0.4926285	MC - 0 , MG - U
kinesin family member 25	KIF25	0.00365427	0.05330912	MC - 0 , MG - U
midkine (neurite growth-promoting factor 2)	MDK	0.00335583	0.47087534	MC - 0 , MG - U
hypothetical protein MGC29643	MGC29643	0.00195104	0.49633509	MC - 0 , MG - U
nuclear factor of kappa light polypeptide gene enhancer in B-cells 2 (p49/p100)	NFKB2	0.00187274	-0.699882	MC - 0 , MG - U
nuclear factor of kappa light polypeptide gene enhancer in B-cells inhibitor, alpha	NFKBIA	0.00120989	-0.2089059	MC - 0 , MG - U
HCV NS3-transactivated protein 2	NS3TP2	0.00000956	1.3889657	MC - 0 , MG - U
phosphodiesterase 9A	PDE9A	0.00014411	0.91583536	MC - 0 , MG - U
protein kinase C substrate 80K-H	PRKCSH	0.00391104	-0.6586338	MC - 0 , MG - U
proteasome (prosome, macropain) subunit, beta type, 8	PSMB8	0.00347777	-0.5075843	MC - 0 , MG - U
polymerase I and transcript release factor	PTRF	0.00001734	0.83480728	MC - 0 , MG - U
RNA binding motif protein 10	RBM10	0.00010017	-0.4896896	MC - 0 , MG - U
RuvB-like 1 (E. coli)	RUVBL1	0.00356509	-0.4197543	MC - 0 , MG - U
serum amyloid A2	SAA2	0.00065689	0.67805246	MC - 0 , MG - U
SH3-domain binding protein 5 (BTK-associated)	SH3BP5	0.00384229	-0.4713608	MC - 0 , MG - U
solute carrier family 21 (organic anion transporter), member 11	SLC21A11	0.00083613	-0.9462162	MC - 0 , MG - U
solute carrier family 25 (mitochondrial carrier: glutamate), member 22	SLC25A22	0.00190172	-0.3400105	MC - 0 , MG - U
solute carrier family 35, member E1	SLC35E1	0.00388026	-0.4350679	MC - 0 , MG - U
tuberous sclerosis 2	TSC2	0.00346356	-0.4842111	MC - 0 , MG - U
vacuolar protein sorting 45A (yeast)	VPS45A	0.00007307	0.27090742	MC - 0 , MG - U
zyxin	ZYX	0.00184693	-0.6202371	MC - 0 , MG - U

Homo sapiens EST from clone 898903, full insert	---	0.00083509	-0.4460085	MC - D , MG - 0
Homo sapiens clone RI-34 thyroid peroxidase autoantibody variable region mRNA	---	0.00066272	-1.2232206	MC - D , MG - 0
Human unidentified mRNA, partial sequence.	---	0.00273167	-0.0843948	MC - D , MG - 0
alpha-2-macroglobulin	A2M	0.00004144	1.18826268	MC - D , MG - 0
ATP-binding cassette, sub-family B (MDR/TAP), member 1	ABCB1	0.00009355	1.19749071	MC - D , MG - 0
ATP-binding cassette, sub-family C (CFTR/MRP), member 5	ABCC5	0.00178395	0.2596241	MC - D , MG - 0
ATP-binding cassette, sub-family G (WHITE), member 2	ABCG2	0.0024482	0.54483994	MC - D , MG - 0
asparaginase like 1	ASRGL1	0.00171947	-0.4322621	MC - D , MG - 0
5-aminoimidazole-4-carboxamide ribonucleotide formyltransferase/IMP cyclohydrolase	ATIC	0.00115125	0.41603815	MC - D , MG - 0
ATPase, Na+/K+ transporting, beta 1 polypeptide	ATP1B1	0.00023958	0.69941947	MC - D , MG - 0
ATPase, Na+/K+ transporting, beta 1 polypeptide	ATP1B1	0.00001282	1.0280713	MC - D , MG - 0
AXL receptor tyrosine kinase	AXL	0.00075057	0.5656772	MC - D , MG - 0
BAI1-associated protein 2	BAIAP2	0.00012535	0.39766611	MC - D , MG - 0
branched chain keto acid dehydrogenase E1, beta polypeptide (maple syrup urine disease)	BCKDHB	0.00044974	0.38332908	MC - D , MG - 0
bullous pemphigoid antigen 1, 230/240kDa	BPAG1	0.0028081	0.81986038	MC - D , MG - 0
CD74(invariant polypeptide, major histocompatibility complex, class II antigen-associated)	CD74	0.00126423	-0.5571805	MC - D , MG - 0
CDW52 antigen (CAMPATH-1 antigen)	CDW52	0.00008905	-1.5959293	MC - D , MG - 0
Charot-Leyden crystal protein	CLC	9.96E-07	-2.0036492	MC - D , MG - 0
C-type lectin, superfamily member 13 (macrophage-derived)	CLECSF13	0.00119258	-1.174893	MC - D , MG - 0
cysteine and glycine-rich protein 2	CSRP2	0.00003886	0.95015396	MC - D , MG - 0
CTP synthase	CTPS	0.0002089	0.47409046	MC - D , MG - 0
chemokine (C-X3-C motif) receptor 1	CX3CR1	0.00193959	-0.9714056	MC - D , MG - 0
drebrin 1	DBN1	0.00107301	0.66167499	MC - D , MG - 0
D component of complement (adipsin)	DF	0.00069455	-0.65679	MC - D , MG - 0
hepatitis delta antigen-interacting protein A	DIPA	0.00127472	0.73347556	MC - D , MG - 0
docking protein 4	DOK4	0.00176188	0.16572436	MC - D , MG - 0
epidermal growth factor receptor (erythroblastic leukemia viral (v-erb-b)	EGFR	0.0002336	0.55179266	MC - D , MG - 0
endothelial PAS domain protein 1	EPAS1	0.00018165	0.55391817	MC - D , MG - 0
epidermal growth factor receptor pathway substrate 8	EPS8	0.00149318	0.73358286	MC - D , MG - 0
FERM, RhoGEF (ARHGEF) and pleckstrin domain protein 1 (chondrocyte-derived)	FARP1	0.00026315	0.91725336	MC - D , MG - 0
FERM, RhoGEF (ARHGEF) and pleckstrin domain protein 1 (chondrocyte-derived)	FARP1	0.00013907	0.90789784	MC - D , MG - 0
fructose-1,6-bisphosphatase 1	FBP1	0.00003446	-0.9816397	MC - D , MG - 0
ficolin (collagen/fibrinogen domain containing) 1	FCN1	1.09E-07	-1.6948655	MC - D , MG - 0
hypothetical protein FLJ12584	FLJ12584	0.00016926	0.76155532	MC - D , MG - 0
hypothetical protein FLJ13110	FLJ13110	0.00041381	0.5047645	MC - D , MG - 0
putative NFkB activating protein 373	FLJ23091	0.00025278	0.66994303	MC - D , MG - 0

growth associated protein 43	GAP43	0.00016401	0.64969693	MC - D , MG - 0
glutamate-cysteine ligase, catalytic subunit	GCLC	0.00045229	0.57320674	MC - D , MG - 0
glutamate-cysteine ligase, catalytic subunit	GCLC	0.00027678	0.83635581	MC - D , MG - 0
guanine nucleotide binding protein (G protein), gamma 11	GNG11	0.00251442	0.64584694	MC - D , MG - 0
G protein-coupled receptor 126	GPR126	0.00257959	0.55037728	MC - D , MG - 0
G protein-coupled receptor, family C, group 5, member B	GPRC5B	0.00038876	0.54816618	MC - D , MG - 0
L-3-hydroxyacyl-Coenzyme A dehydrogenase, short chain	HADHSC	0.00369993	0.49140299	MC - D , MG - 0
hemoglobin, alpha 1	HBA1	0.00000263	-2.0788735	MC - D , MG - 0
hemoglobin, alpha 1	HBA1	0.00000727	-1.8058066	MC - D , MG - 0
hemoglobin, alpha 1	HBA1	6.37E-07	-2.0543247	MC - D , MG - 0
hemoglobin, alpha 1	HBA1	1.53E-07	-1.8670227	MC - D , MG - 0
hemoglobin, beta	HBB	0.00000177	-2.3228371	MC - D , MG - 0
hemoglobin, beta	HBB	0.00000503	-1.7427576	MC - D , MG - 0
major histocompatibility complex, class II, DM alpha	HLA-DMA	0.00320966	-0.5025173	MC - D , MG - 0
major histocompatibility complex, class II, DP alpha 1	HLA-DPA1	0.00321274	-0.7189745	MC - D , MG - 0
major histocompatibility complex, class II, DP alpha 1	HLA-DPA1	0.00004911	-0.9541136	MC - D , MG - 0
major histocompatibility complex, class II, DP beta 1	HLA-DPB1	0.00001204	-0.8336442	MC - D , MG - 0
major histocompatibility complex, class II, DQ alpha 1	HLA-DQA1	0.00292942	-1.1884326	MC - D , MG - 0
major histocompatibility complex, class II, DQ alpha 1	HLA-DQA1	0.00028943	-1.3890141	MC - D , MG - 0
major histocompatibility complex, class II, DQ beta 1	HLA-DQB1	0.00166327	-1.081308	MC - D , MG - 0
major histocompatibility complex, class II, DQ beta 1	HLA-DQB1	5.01E-08	-1.124174	MC - D , MG - 0
major histocompatibility complex, class II, DQ beta 1	HLA-DQB1	0.00179703	-0.7402938	MC - D , MG - 0
major histocompatibility complex, class II, DQ beta 2	HLA-DQB2	0.000121	-1.3134924	MC - D , MG - 0
major histocompatibility complex, class II, DR beta 3	HLA-DRB3	0.00003015	-0.8961618	MC - D , MG - 0
major histocompatibility complex, class II, DR beta 3	HLA-DRB3	0.0002507	-0.9170904	MC - D , MG - 0
major histocompatibility complex, class II, DR beta 3	HLA-DRB3	0.00009957	-1.034621	MC - D , MG - 0
major histocompatibility complex, class II, DR beta 3	HLA-DRB3	0.00007592	-1.1655578	MC - D , MG - 0
major histocompatibility complex, class II, DR beta 3	HLA-DRB3	0.00050215	-0.8284418	MC - D , MG - 0
hydroxymethylbilane synthase	HMBS	0.00201883	-0.1974628	MC - D , MG - 0
heparan sulfate (glucosamine) 3-O-sulfotransferase 2	HS3ST2	0.00024689	-0.3728932	MC - D , MG - 0
immunoglobulin heavy constant gamma 3 (G3m marker)	IGHG3	0.00000656	-2.254905	MC - D , MG - 0
immunoglobulin lambda locus	IGL@	3.71E-07	-1.8015584	MC - D , MG - 0
immunoglobulin lambda joining 3	IGLJ3	6.55E-08	-2.3831532	MC - D , MG - 0
immunoglobulin superfamily, member 4	IGSF4	0.00129754	1.1719131	MC - D , MG - 0
interleukin 13 receptor, alpha 2	IL13RA2	0.00054932	0.90714185	MC - D , MG - 0
IGF-II mRNA-binding protein 3	IMP-3	0.00027253	1.10748446	MC - D , MG - 0

inositol polyphosphate-4-phosphatase, type II, 105kDa	INPP4B	0.00294067	0.52133834	MC - D , MG - 0
potassium large conductance calcium-activated channel, subfamily M, alpha member 1	KCNMA1	0.00007182	0.89168592	MC - D , MG - 0
KH domain containing, RNA binding, signal transduction associated 3	KHDRBS3	0.00116987	0.7316471	MC - D , MG - 0
kinesin family member 23	KIF23	0.00343644	0.59062205	MC - D , MG - 0
leptin (obesity homolog, mouse)	LEP	0.00048745	-0.8169255	MC - D , MG - 0
legumain	LGMN	0.0010821	0.54250872	MC - D , MG - 0
lipase A, lysosomal acid, cholesterol esterase (Wolman disease)	LIPA	0.00188557	0.38102183	MC - D , MG - 0
lymphocyte antigen 9	LY9	0.00212935	-0.464366	MC - D , MG - 0
hypothetical protein MAC30	MAC30	0.00267682	0.63759511	MC - D , MG - 0
mitogen-activated protein kinase kinase kinase kinase 1	MAP4K1	0.00219993	-0.4075711	MC - D , MG - 0
MADS box transcription enhancer factor 2, polypeptide C (myocyte enhancer factor 2C)	MEF2C	0.00044431	0.38502338	MC - D , MG - 0
esophageal cancer associated protein	MGC16824	0.00056605	0.49670462	MC - D , MG - 0
microsomal glutathione S-transferase 2	MGST2	0.00022408	0.59164542	MC - D , MG - 0
MHC class II transactivator	MHC2TA	0.00029127	-0.4886218	MC - D , MG - 0
myeloid leukemia factor 1	MLF1	0.00008063	1.28468229	MC - D , MG - 0
mannose receptor, C type 1	MRC1	0.00001443	0.84720277	MC - D , MG - 0
mannose receptor, C type 2	MRC2	0.00012139	0.97113259	MC - D , MG - 0
membrane-spanning 4-domains, subfamily A, member 3 (hematopoietic cell-specific)	MS4A3	0.00219203	-0.9375864	MC - D , MG - 0
neurofilament, heavy polypeptide 200kDa	NEFH	0.00246112	0.98372453	MC - D , MG - 0
prostatic binding protein	PBP	0.00303582	0.59778247	MC - D , MG - 0
phytanoyl-CoA hydroxylase (Refsum disease)	PHYH	0.00200378	0.28544344	MC - D , MG - 0
polycystic kidney disease 2-like 1	PKD2L1	6.64E-07	0.66922238	MC - D , MG - 0
paraoxonase 2	PON2	0.00055905	0.67970881	MC - D , MG - 0
POU domain, class 2, associating factor 1	POU2AF1	0.00087823	-0.9192306	MC - D , MG - 0
phosphatidic acid phosphatase type 2B	PPAP2B	0.00162568	-0.7505307	MC - D , MG - 0
protein kinase, cAMP-dependent, catalytic, beta	PRKACB	0.00193854	0.12563276	MC - D , MG - 0
pleiotrophin (heparin binding growth factor 8, neurite growth-promoting factor 1)	PTN	0.00109669	1.06909054	MC - D , MG - 0
quinolinate phosphoribosyltransferase (nicotinate-nucleotide pyrophosphorylase	QPRT	0.0000229	1.54134661	MC - D , MG - 0
NADP-dependent retinol dehydrogenase/reductase	RDHL	0.00115596	-0.1956371	MC - D , MG - 0
ribonuclease P1	RNASEP1	0.00113459	0.33944913	MC - D , MG - 0
sterile alpha motif domain containing 4	SAMD4	0.00000691	0.94540944	MC - D , MG - 0
sterile alpha motif domain containing 4	SAMD4	0.00039786	0.50779695	MC - D , MG - 0
stromal cell-derived factor 2-like 1	SDF2L1	0.00181154	-0.4470649	MC - D , MG - 0
semaphorin 4F	SEMA4F	0.00276847	0.29085484	MC - D , MG - 0
selenoprotein P, plasma, 1	SEPP1	0.00002574	0.94246322	MC - D , MG - 0
serine (or cysteine) proteinase inhibitor, clade E nexin, plasminogen activator inhibitor 1	SERPINE1	0.00284799	0.76988111	MC - D , MG - 0

sialic acid binding Ig-like lectin 8	SIGLEC8	0.0013343	1.32699491	MC - D , MG - 0
solute carrier family 25 (mitochondrial carrier; adenine nucleotide translocator)	SLC25A5	0.00150383	0.38911873	MC - D , MG - 0
solute carrier family 28 (sodium-coupled nucleoside transporter), member 1	SLC28A1	0.00135938	0.17047844	MC - D , MG - 0
SMP3 mannosyltransferase	SMP3	0.00080391	-0.1115424	MC - D , MG - 0
sorting nexin 7	SNX7	0.00240239	0.7611859	MC - D , MG - 0
stathmin 1/oncoprotein 18	STMN1	0.00036079	0.46107042	MC - D , MG - 0
sulfotransferase family, cytosolic, 1C, member 1	SULT1C1	0.00059207	1.04104201	MC - D , MG - 0
translocase of inner mitochondrial membrane 17 homolog A (yeast)	TIMM17A	0.0001912	0.34464466	MC - D , MG - 0
transmembrane 4 superfamily member 10	TM4SF10	0.00012343	0.894098	MC - D , MG - 0
class I cytokine receptor	WSX1	0.00074872	-1.2311147	MC - D , MG - 0
ankylosis, progressive homolog (mouse)	ANKH	0.0015023	-0.1800579	MC - D , MG - D
CDW52 antigen (CAMPATH-1 antigen)	CDW52	0.00065473	-1.5468382	MC - D , MG - D
coronin, actin binding protein, 2B	CORO2B	0.00106216	0.38355254	MC - D , MG - D
hypothetical protein FLJ20581	FLJ20581	0.00002679	1.35551729	MC - D , MG - D
growth hormone 1	GH1	0.00092771	-0.0719208	MC - D , MG - D
hemoglobin, alpha 1	HBA1	0.00000153	-2.4681509	MC - D , MG - D
chromosome condensation protein G	HCAP-G	0.00255094	0.60730403	MC - D , MG - D
major histocompatibility complex, class II, DQ beta 1	HLA-DQB1	0.00131574	-1.157595	MC - D , MG - D
major histocompatibility complex, class II, DQ beta 1	HLA-DQB1	0.00067709	-1.1507943	MC - D , MG - D
hypothetical protein MGC27165	MGC27165	1.07E-07	-2.5482453	MC - D , MG - D
macrophage scavenger receptor 1	MSR1	0.00010479	1.37976655	MC - D , MG - D
phosphodiesterase 11A	PDE11A	0.00229325	0.31496629	MC - D , MG - D
prostaglandin D2 synthase, hematopoietic	PGDS	0.00045056	1.12957094	MC - D , MG - D
Rho-related BTB domain containing 1	RHOBTB1	0.00004196	1.08168333	MC - D , MG - D
triggering receptor expressed on myeloid cells 2	TREM2	0.0002362	0.81373836	MC - D , MG - D
tripartite motif-containing 2	TRIM2	0.00153486	0.24175799	MC - D , MG - D
Fc fragment of IgE, high affinity I, receptor for; alpha polypeptide	FCER1A	0.00003549	-1.2741277	MC - D , MG - U
interleukin 1 receptor, type II	IL1R2	0.00007644	-1.0578372	MC - D , MG - U
syndecan 1	SDC1	0.00000294	0.83295653	MC - D , MG - U
Homo sapiens transcribed sequences	---	0.00152295	0.36744648	MC - U , MG - 0
Homo sapiens mRNA, chromosome 1 specific transcript KIAA0500.	---	0.00050032	-0.9964484	MC - U , MG - 0
actin, alpha 2, smooth muscle, aorta	ACTA2	0.00012457	0.34395204	MC - U , MG - 0
a disintegrin and metalloproteinase domain 28	ADAM28	0.00003769	0.59891417	MC - U , MG - 0
adenylate kinase 3	AK3	0.00101091	-0.720284	MC - U , MG - 0
adenylate kinase 3	AK3	0.00044206	-0.7927381	MC - U , MG - 0
aldolase C, fructose-bisphosphate	ALDOC	0.00297454	-0.6499269	MC - U , MG - 0

alanyl aminopeptidase	ANPEP	0.0011957	-0.9233053	MC - U , MG - 0
arginase, type II	ARG2	0.00006877	1.0932315	MC - U , MG - 0
activating transcription factor 5	ATF5	0.00023312	-0.4814143	MC - U , MG - 0
activating transcription factor 5	ATF5	0.00106797	-0.6859113	MC - U , MG - 0
B-cell CLL/lymphoma 3	BCL3	0.00049325	-0.2971643	MC - U , MG - 0
BRAF35/HDAC2 complex (80 kDa)	BHC80	0.00077054	-0.2110392	MC - U , MG - 0
complement component 1, q subcomponent, receptor 1	C1QR1	0.00003273	-0.46027	MC - U , MG - 0
complement component 3	C3	0.00013626	1.51708461	MC - U , MG - 0
caldesmon 1	CALD1	0.00093446	0.9220844	MC - U , MG - 0
caveolin 1, caveolae protein, 22kDa	CAV1	0.00068232	1.20962279	MC - U , MG - 0
chemokine (C-C motif) receptor 2	CCR2	0.00020548	-1.3123286	MC - U , MG - 0
chemokine (C-C motif) receptor 2	CCR2	0.00100727	-0.6014681	MC - U , MG - 0
CD44 antigen (homing function and Indian blood group system)	CD44	0.00346497	-0.4458147	MC - U , MG - 0
cytidine deaminase	CDA	0.00124354	-1.0488606	MC - U , MG - 0
CDC42 effector protein (Rho GTPase binding) 2	CDC42EP2	0.00066419	0.00462243	MC - U , MG - 0
CASP8 and FADD-like apoptosis regulator	CFLAR	0.00220795	-0.268824	MC - U , MG - 0
CASP8 and FADD-like apoptosis regulator	CFLAR	0.0009442	-0.3166975	MC - U , MG - 0
chloride channel 4	CLCN4	0.00014916	0.97496512	MC - U , MG - 0
chondroitin sulfate proteoglycan 2 (versican)	CSPG2	0.00250936	-1.1595098	MC - U , MG - 0
chondroitin sulfate proteoglycan 2 (versican)	CSPG2	0.00141785	-1.1723074	MC - U , MG - 0
chondroitin sulfate proteoglycan 2 (versican)	CSPG2	0.00306579	-1.3703968	MC - U , MG - 0
chondroitin sulfate proteoglycan 2 (versican)	CSPG2	0.00206361	-1.3315782	MC - U , MG - 0
cytochrome P450, family 39, subfamily A, polypeptide 1	CYP39A1	0.0003926	0.66839941	MC - U , MG - 0
hypothetical protein DKFZp434K1210	DKFZp434K1210	0.00098444	-1.0419332	MC - U , MG - 0
dickkopf homolog 3 (Xenopus laevis)	DKK3	0.00366536	1.24326897	MC - U , MG - 0
dystrobrevin, beta	DTNB	0.0004933	0.44024475	MC - U , MG - 0
diphtheria toxin receptor (heparin-binding epidermal growth factor-like growth factor)	DTR	0.00007857	0.52743071	MC - U , MG - 0
endothelin receptor type B	EDNRB	0.00000274	0.79918756	MC - U , MG - 0
endothelin receptor type B	EDNRB	0.00232521	0.36720145	MC - U , MG - 0
likely ortholog of mouse embryonic epithelial gene 1	EEG1	0.0002572	-0.5319741	MC - U , MG - 0
ephrin-B2	EFNB2	0.00000485	0.81393085	MC - U , MG - 0
ERO1-like (S. cerevisiae)	ERO1L	0.0031406	-0.1339116	MC - U , MG - 0
ets variant gene 5 (ets-related molecule)	ETV5	0.00000322	0.69454289	MC - U , MG - 0
Fc fragment of IgA, receptor for	FCAR	0.00357775	-0.6842739	MC - U , MG - 0
hypothetical protein FLJ10539	FLJ10539	0.0026246	0.83799807	MC - U , MG - 0
hypothetical protein FLJ12377	FLJ12377	0.00066297	0.6321724	MC - U , MG - 0

hypothetical protein FLJ20701	FLJ20701	0.00012272	-1.5462029	MC - U , MG - 0
formyl peptide receptor-like 1	FPRL1	0.00245971	-0.4136035	MC - U , MG - 0
GABA(A) receptors associated protein like 3	GABARAPL3	0.00223779	0.21178371	MC - U , MG - 0
beta-galactose-3-O-sulfotransferase, 4	GAL3ST-4	0.00000837	1.4192731	MC - U , MG - 0
glycerol kinase	GK	0.00244286	-0.0756302	MC - U , MG - 0
guanine nucleotide binding protein (G protein), alpha 15 (Gq class)	GNA15	0.00021285	-0.2907258	MC - U , MG - 0
glutamate receptor, metabotropic 1	GRM1	0.00218037	0.43597237	MC - U , MG - 0
glycogen synthase 1 (muscle)	GYS1	0.00063712	-0.310931	MC - U , MG - 0
heat shock 70kDa protein 6 (HSP70B')	HSPA6	0.00026722	-0.6870426	MC - U , MG - 0
inhibitor of kappa light polypeptide gene enhancer in B-cells, kinase epsilon	IKBKE	0.00114791	-0.1024103	MC - U , MG - 0
inhibitor of growth family, member 1	ING1	0.00028653	0.60583117	MC - U , MG - 0
integrin, b 1 (fibronectin receptor, beta polypeptide, antigen CD29 includes MDF2, MSK12)	ITGB1	0.00357137	0.19303287	MC - U , MG - 0
jagged 1 (Alagille syndrome)	JAG1	0.00022281	0.52813634	MC - U , MG - 0
potassium inwardly-rectifying channel, subfamily J, member 15	KCNJ15	0.0003342	-0.7933123	MC - U , MG - 0
potassium inwardly-rectifying channel, subfamily J, member 15	KCNJ15	0.00005539	-0.5164348	MC - U , MG - 0
KIAA0876 protein	KIAA0876	0.00126027	-0.6916524	MC - U , MG - 0
kinesin family member 20A	KIF20A	0.00001589	0.8607011	MC - U , MG - 0
laminin, beta 3	LAMB3	0.00256245	-0.1007989	MC - U , MG - 0
laminin, gamma 1 (formerly LAMB2)	LAMC1	0.00003745	0.50804747	MC - U , MG - 0
lysosomal-associated membrane protein 3	LAMP3	0.00383632	-0.8962456	MC - U , MG - 0
lymphocyte cytosolic protein 1 (L-plastin)	LCP1	0.0014927	-0.4562166	MC - U , MG - 0
leukocyte immunoglobulin-like receptor, subfamily B (with TM and ITIM domains), member 1	LILRB1	0.00124016	-0.570694	MC - U , MG - 0
leukocyte immunoglobulin-like receptor, subfamily B (with TM and ITIM domains), member 1	LILRB1	0.00136991	-0.5786955	MC - U , MG - 0
leukocyte Ig-like receptor 9	LIR9	0.00021564	-0.4606308	MC - U , MG - 0
stromal cell protein	LOC55974	0.00098503	-0.1458599	MC - U , MG - 0
monoamine oxidase A	MAOA	0.00187775	0.9726867	MC - U , MG - 0
monoamine oxidase A	MAOA	0.00393337	0.94602773	MC - U , MG - 0
c-mer proto-oncogene tyrosine kinase	MERTK	0.0031174	0.51695584	MC - U , MG - 0
met proto-oncogene (hepatocyte growth factor receptor)	MET	0.00008193	0.05221977	MC - U , MG - 0
hypothetical protein MGC25062	MGC25062	0.00316572	1.34979502	MC - U , MG - 0
macrophage migration inhibitory factor (glycosylation-inhibiting factor)	MIF	0.00085617	-0.5414905	MC - U , MG - 0
mitochondrial solute carrier protein	MSCP	0.00154317	-0.3359498	MC - U , MG - 0
NACHT, LRR and PYD containing protein 2	NALP2	0.00057339	0.81998927	MC - U , MG - 0
N-myc downstream regulated gene 1	NDRG1	0.00009923	-0.5979941	MC - U , MG - 0
neurofibromin 1 (neurofibromatosis, von Recklinghausen disease, Watson disease)	NF1	0.00157104	0.28951944	MC - U , MG - 0
nuclear receptor subfamily 2, group F, member 2	NR2F2	0.0031759	0.78418293	MC - U , MG - 0

odd Oz/ten-m homolog 4	ODZ4	0.00236964	0.84909237	MC - U , MG - 0
pyrimidinergic receptor P2Y, G-protein coupled, 6	P2RY6	0.00287685	0.23872864	MC - U , MG - 0
papillomavirus regulatory factor PRF-1	PBF	0.00102777	-1.2580829	MC - U , MG - 0
6-phosphofructo-2-kinase/fructose-2,6-biphosphatase 4	PFKFB4	0.00211791	-0.3395489	MC - U , MG - 0
pleckstrin homology domain containing, family C (with FERM domain) member 1	PLEKHC1	0.00028466	1.22643759	MC - U , MG - 0
proteolipid protein 2 (colonic epithelium-enriched)	PLP2	0.00017165	-0.5904562	MC - U , MG - 0
protein S (alpha)	PROS1	0.00000433	0.69148407	MC - U , MG - 0
prostaglandin I2 (prostacyclin) receptor (IP)	PTGIR	0.0000042	-1.2099681	MC - U , MG - 0
protein tyrosine phosphatase, non-receptor type 1	PTPN1	0.00153578	-0.3388252	MC - U , MG - 0
protein tyrosine phosphatase, non-receptor type 2	PTPN2	0.00195107	-0.1327782	MC - U , MG - 0
poliovirus receptor-related 2 (herpesvirus entry mediator B)	PVRL2	0.00004327	-0.1619277	MC - U , MG - 0
RAB27A, member RAS oncogene family	RAB27A	0.00114687	-0.5240811	MC - U , MG - 0
rabconnectin-3	RC3	0.00092978	-0.5000581	MC - U , MG - 0
G protein-coupled receptor	RDC1	0.00349846	-0.7687846	MC - U , MG - 0
ribonuclease, RNase A family, 4	RNASE4	0.00374871	-0.6150549	MC - U , MG - 0
HIF-1 responsive RTP801	RTP801	0.00084938	-0.0222899	MC - U , MG - 0
retinoid X receptor, alpha	RXRA	0.00009083	-0.479461	MC - U , MG - 0
S100 calcium binding protein A12 (calgranulin C)	S100A12	0.00101431	-0.6520719	MC - U , MG - 0
semaphorin 4C	SEMA4C	0.00018727	0.62737052	MC - U , MG - 0
serine (or cysteine) proteinase inhibitor, clade B (ovalbumin), member 2	SERPINB2	0.00056206	-0.9187999	MC - U , MG - 0
solute carrier family 11 (proton-coupled divalent metal ion transporters), member 1	SLC11A1	0.00001764	-0.5227271	MC - U , MG - 0
solute carrier family 11 (proton-coupled divalent metal ion transporters), member 1	SLC11A1	0.00001072	-0.6164177	MC - U , MG - 0
solute carrier family 2 (facilitated glucose transporter), member 14	SLC2A14	0.00072751	-0.3081214	MC - U , MG - 0
solute carrier family 2 (facilitated glucose transporter), member 14	SLC2A14	0.00098325	-0.5772709	MC - U , MG - 0
solute carrier family 2 (facilitated glucose transporter), member 3	SLC2A3	0.00010154	-0.2336899	MC - U , MG - 0
suppressor of cytokine signaling 3	SOCS3	0.00035589	-0.373791	MC - U , MG - 0
suppressor of cytokine signaling 3	SOCS3	0.00307102	-0.2564336	MC - U , MG - 0
superoxide dismutase 2, mitochondrial	SOD2	0.00214423	-0.4239649	MC - U , MG - 0
lung type-I cell membrane-associated glycoprotein	T1A-2	0.00009866	0.83265927	MC - U , MG - 0
transforming growth factor, beta 2	TGFB2	0.00328175	0.33532991	MC - U , MG - 0
tenascin C (hexabrachion)	TNC	0.00279099	0.90182908	MC - U , MG - 0
tumor necrosis factor receptor superfamily, member 1B	TNFRSF1B	0.00120295	-0.3511801	MC - U , MG - 0
tumor necrosis factor receptor superfamily, member 8	TNFRSF8	0.00001876	-0.6483724	MC - U , MG - 0
triosephosphate isomerase 1	TPI1	0.000775	-0.2384197	MC - U , MG - 0
triosephosphate isomerase 1	TPI1	0.00206009	-0.296162	MC - U , MG - 0
triggering receptor expressed on myeloid cells 1	TREM1	0.0006918	-0.9615129	MC - U , MG - 0

thyroid hormone receptor interactor 10	TRIP10	0.00300765	-0.1803162	MC - U , MG - 0
vascular endothelial growth factor	VEGF	0.00199755	-0.7262579	MC - U , MG - 0
vascular endothelial growth factor	VEGF	0.00000774	-0.6164426	MC - U , MG - 0
vascular endothelial growth factor	VEGF	0.00007463	-0.424073	MC - U , MG - 0
wingless-type MMTV integration site family, member 5A	WNT5A	0.0004911	1.24383515	MC - U , MG - 0
zinc finger protein 36, C3H type-like 1	ZFP36L1	0.00093628	-0.7305477	MC - U , MG - 0
chondroitin sulfate proteoglycan 2 (versican)	CSPG2	0.0010774	-1.5169779	MC - U , MG - D
chemokine (C-X-C motif) ligand 13 (B-cell chemoattractant)	CXCL13	0.00023891	-0.5870241	MC - U , MG - D
dystrobrevin, alpha	DTNA	0.00312839	-0.0822651	MC - U , MG - D
egf-like module containing, mucin-like, hormone receptor-like sequence 2	EMR2	0.00023783	-0.9590764	MC - U , MG - D
KIAA1199 protein	KIAA1199	0.00160545	-0.5349299	MC - U , MG - D
myeloperoxidase	MPO	0.00081795	-0.5878718	MC - U , MG - D
Homo sapiens mitochondrial ribosomal protein L4	---	0.00003434	-0.1923318	MC - U , MG - U
Homo sapiens PRO2275 mRNA, complete cds	---	0.00002888	-0.8564496	MC - U , MG - U
Homo sapiens similar to neutrophil cytosolic factor 1	---	0.00200554	-0.1138678	MC - U , MG - U
adenosine deaminase	ADA	0.00063906	-0.2279878	MC - U , MG - U
adenosine deaminase	ADA	0.0008161	-0.3527255	MC - U , MG - U
adrenomedullin	ADM	0.0015136	-0.2371905	MC - U , MG - U
adenosine A2a receptor	ADORA2A	0.00327037	-0.4588637	MC - U , MG - U
chemokine (C-C motif) receptor 7	CCR7	0.0009183	-0.9122107	MC - U , MG - U
EH-domain containing 1	EHD1	0.00020108	-0.0368307	MC - U , MG - U
egf-like module containing, mucin-like, hormone receptor-like sequence 1	EMR1	0.00004244	0.09862715	MC - U , MG - U
hypothetical protein FLJ23231	FLJ23231	0.00044998	-0.3588363	MC - U , MG - U
putative lymphocyte G0/G1 switch gene	G0S2	0.00024279	-0.788295	MC - U , MG - U
hepatocellular carcinoma-associated antigen 112	HCA112	0.00079974	0.45044089	MC - U , MG - U
hemopoietic cell kinase	HCK	0.00001546	-0.1898823	MC - U , MG - U
interleukin-1 receptor-associated kinase 3	IRAK3	0.00314088	-0.1885261	MC - U , MG - U
leukocyte immunoglobulin-like receptor, subfamily A (without TM domain), member 3	LILRA3	0.00026193	-0.7493495	MC - U , MG - U
leukocyte immunoglobulin-like receptor, subfamily B (with TM and ITIM domains), member 1	LILRB1	0.00032975	-0.8914426	MC - U , MG - U
leukocyte immunoglobulin-like receptor, subfamily B (with TM and ITIM domains), member 1	LILRB1	0.00064164	-0.2432381	MC - U , MG - U
leukocyte immunoglobulin-like receptor, subfamily B (with TM and ITIM domains), member 2	LILRB2	0.0004026	-0.2983453	MC - U , MG - U
leukocyte immunoglobulin-like receptor, subfamily B (with TM and ITIM domains), member 3	LILRB3	0.00221035	-0.5185599	MC - U , MG - U
leukocyte immunoglobulin-like receptor, subfamily B (with TM and ITIM domains), member 3	LILRB3	0.00355718	-0.268582	MC - U , MG - U
leukocyte immunoglobulin-like receptor, subfamily B (with TM and ITIM domains), member 3	LILRB3	0.00120721	-0.2921946	MC - U , MG - U
leukocyte immunoglobulin-like receptor, subfamily B (with TM and ITIM domains), member 3	LILRB3	0.00102466	-0.3216662	MC - U , MG - U
LIM domain kinase 2	LIMK2	0.00149486	-0.0189591	MC - U , MG - U

LIM domain kinase 2	LIMK2	0.00024494	-0.19125	MC - U , MG - U
LR8 protein	LR8	0.00016435	0.21808694	MC - U , MG - U
macrophage receptor with collagenous structure	MARCO	0.00015829	-1.499451	MC - U , MG - U
hypothetical protein MGC16353	MGC16353	0.00031548	-0.9384321	MC - U , MG - U
matrix metalloproteinase 14 (membrane-inserted)	MMP14	0.00248243	0.45037006	MC - U , MG - U
mitochondrial solute carrier protein	MSCP	0.00044883	-0.4993884	MC - U , MG - U
pyruvate kinase, muscle	PKM2	0.00174703	-0.3093279	MC - U , MG - U
phospholipid transfer protein	PLTP	0.00096076	1.32268718	MC - U , MG - U
Ras-induced senescence 1	RIS1	0.00016878	0.99161436	MC - U , MG - U
related RAS viral (r-ras) oncogene homolog	RRAS	0.00036067	-0.4930141	MC - U , MG - U
S100 calcium binding protein A9 (calgranulin B)	S100A9	0.00000558	-0.6440196	MC - U , MG - U
serine (or cysteine) proteinase inhibitor, clade A (alpha-1 antiproteinase, antitrypsin), 1	SERPINA1	0.00000775	-0.8953174	MC - U , MG - U
sialyltransferase 4A (beta-galactoside alpha-2,3-sialyltransferase)	SIAT4A	0.00169675	-0.2921762	MC - U , MG - U
solute carrier family 16 (monocarboxylic acid transporters), member 10	SLC16A10	0.00328364	-0.4276887	MC - U , MG - U
lung type-I cell membrane-associated glycoprotein	T1A-2	0.00003033	0.86982987	MC - U , MG - U
thrombospondin 1	THBS1	0.00101556	-1.2576039	MC - U , MG - U
tissue inhibitor of metalloproteinase 1 (erythroid potentiating activity, collagenase inhibitor)	TIMP1	0.00001563	-0.4679792	MC - U , MG - U
toll-like receptor 2	TLR2	0.00222957	0.16862741	MC - U , MG - U
tumor necrosis factor, alpha-induced protein 3	TNFAIP3	0.00185745	-0.1228505	MC - U , MG - U
TNFAIP3 interacting protein 1	TNIP1	0.00187853	-0.1932694	MC - U , MG - U

Supplementary Table S2: Primers and probes.

TLR1	
sense:	5’-CCACAACAAGTTGGTGAAGATTTCT-3’
antisense	5’-GCATATAGGCAGGGCATCAAATG-3’
probe:	5’-ACTGTGAACCTCAAGCACTTGGACCTGTCA-3’
TLR2	
sense:	5’-TTCAGGATGTCCGCCTCTCG-3’
antisense:	5’-CCCGTGAGCAGGATCAGCA-3’
probe:	5’-ACAGAGCACAGCACATGCCAGACACCA-3’
TLR4	
sense:	5’-AAAGCCGAAAGGTGATTGTTGTG-3’
antisense:	5’-TGCTCAGAAACTGCCAGGTCT-3’
probe:	5’-TGTCCCAGCACTTCATCCAGAGCCGC-3’
TLR6	
sense:	5’-GAAGAAGAACAACCCTTTAGGATAGC-3’
antisense:	5’-GCTGGATTCTGTTATGGGAAAGTC-3’
probe:	5’-CAAAAAGACCTACCGCTGAAAACCAAAGTC-3’
MyD88	
sense:	5’-CTCCTCCACATCCTCCCTTCC-3’
antisense:	5’-CGCACGTTCAAGAACAGAGACA-3’
probe:	5’CCGCACTCGCATGTTGAGAGCAGCCAG-3’